

# 1 A Novel Variable Neighborhood Search Approach for Cell Clustering for Spatial 2 Transcriptomics

3

## 4 Authors:

5 Aleksandra Djordjevic<sup>1,\*</sup>, [aleksandradjordjevic@genomics.cn](mailto:aleksandradjordjevic@genomics.cn)

6 Junhua Li<sup>1,3</sup>, [lijunhua@genomics.cn](mailto:lijunhua@genomics.cn)

7 Shuangfang Fang<sup>1,2</sup>, [fangshuangfang@genomics.cn](mailto:fangshuangfang@genomics.cn)

8 Lei Cao<sup>1,2</sup>, [caolei2@genomics.cn](mailto:caolei2@genomics.cn)

9 Marija Ivanovic<sup>1,\*</sup>, [marijaivanovic@genomics.cn](mailto:marijaivanovic@genomics.cn)

10

11 1 BGI Research, Shenzhen 518083, China

12 2 BGI Research, Beijing 102601, China

13 3 BGI Research, Lidostas Parks, Riga 49276, Latvia

14

15 \* contributed equally, corresponding authors.

16 ORCID IDs:

17 Marija Ivanovic [0000-0002-3372-8271], Aleksandra Djordjevic [0009-0002-9450-4121], Junhua Li  
18 [0000-0001-6784-1873], Shuangfang Fang [0000-0002-4126-0074], Lei Cao [0000-0002-7170-9602];

19

## 20 Abstract

21 This paper introduces a new approach to cell clustering using the Variable Neighborhood Search (VNS)  
22 metaheuristic. The purpose of this method is to cluster cells based on both gene expression and spatial  
23 coordinates. Initially, we confronted this clustering challenge as an Integer Linear Programming  
24 minimization problem. Our approach introduced a novel model based on the VNS technique,  
25 demonstrating the efficacy in navigating the complexities of cell clustering. Notably, our method  
26 extends beyond conventional cell-type clustering to spatial domain clustering. This adaptability  
27 enables our algorithm to orchestrate clusters based on information gleaned from gene expression  
28 matrices and spatial coordinates. Our validation showed the superior performance of our method  
29 when compared to existing techniques. Our approach advances current clustering methodologies and  
30 can potentially be applied to several fields, from biomedical research to spatial data analysis.

31 **Subject areas:** Software and Workflows, Bioinformatics, Transcriptomics.

32

## 33 Statement of Need

34

35 In high-throughput omics, deciphering the intricate cellular dynamics within tissues is pivotal  
36 [1,2]. Cell clustering is essential for dissecting the mosaic of cellular diversity [3,4]. This analytical  
37 approach seeks to categorize individual cells based on shared molecular signatures, allowing the  
38 identification of discrete subpopulations within heterogeneous tissues. In exploring cellular behavior  
39 and function, cell clustering emerges as an indispensable tool, providing insights into the subtle  
40 nuances of gene expression profiles. The ability to stratify cells into meaningful clusters not only refines

41 our understanding of tissue composition but also lays the groundwork for precise insights into disease  
42 etiology and potential therapeutic interventions.

43 In tandem with cell clustering, spatial transcriptomics [5,6] constitutes a revolutionary frontier  
44 for understanding cellular dynamics with their native microenvironments. Beyond the traditional  
45 scope of genomics, spatial transcriptomics integrates the spatial context of cells into the analysis,  
46 allowing researchers to explore how gene expression patterns unfold across complex tissue structures.  
47 This multidimensional approach surpasses the limitations of conventional transcriptomic studies,  
48 providing a spatially resolved perspective that is indispensable for decoding the orchestration of  
49 cellular interactions and the emergence of tissue-specific functions.

50 In order to contribute to this dynamic landscape, we introduce a novel methodology rooted in  
51 the Variable Neighborhood Search approach [7]. Our innovation seeks to elevate the precision and  
52 efficacy of cell clustering in spatial transcriptomic analyses, promising to reveal hidden facets of cellular  
53 organization and functionality. In this work, we introduce a novel Variable Neighborhood Search (VNS)  
54 approach tailored for cell clustering in spatial transcriptomics. Although our initial investigations  
55 focused on datasets designed for cell-type clustering, it is essential to emphasize that our method's  
56 design accommodates spatial domain clustering as well. Here, we present a synthesis of computational  
57 skills and biological insights aimed at pushing the boundaries of our understanding of the complex cell  
58 interactions within tissues.

59

## 60 Background

### 61 Clustering methods from the literature

62

63 Many methods in the literature can be used to partition an  $N$ -dimensional population into  $K$  sets  
64 based on specific rules. In this paper, we focus on some of the most popular clustering methods used  
65 in the field of data analysis, such as  $k$ -Means [8], Louvain [9], Leiden [10], and MClust [11]. While these  
66 methods share the goal of grouping data points, they differ in the types of data they are designed for,  
67 the principle they optimize, and the algorithms they are well-suited for.  $k$ -Means is a general-purpose  
68 clustering algorithm, Louvain and Leiden are tailored for community detection in networks, while  
69 MClust is a model-based clustering method. In the following subsections, we briefly describe each of  
70 these methods.

71

#### 72 *k*-Means algorithm

73 The  $k$ -means algorithm [8] is a partitioning algorithm that divides a dataset into  $k$ -clusters based on  
74 the similarity of data points. It starts by establishing  $k$  groups, each comprising a singular randomly  
75 chosen point. Points are then added to these groups according to the principle that new points are  
76 assigned to the group whose mean point is the most similar by some rule. After point allocation, the  
77 means of all groups are adjusted to incorporate the influence of newly added points. Consequently, at  
78 each stage, the  $k$ -means are reflective of the means of the groups they represent.

79 While this method is computationally efficient and adeptly handles extensive datasets, it does  
80 not guarantee convergence to an optimal solution. Notably, issues arise from the random initialization  
81 of centroids, leading to unexpected convergence patterns. Moreover, the algorithm requires users to  
82 choose the cluster number beforehand, influencing cluster shapes and susceptibility to outlier effects.  
83 However, it is known that certain special cases of the  $k$ -means algorithm exist in the literature where  
84 convergence to an optimal solution is assured.

85

## 86 *Louvain algorithm*

87 The Louvain algorithm, developed by V. D. Vondel et al. [9], is designed for detecting communities in  
88 network or graph data. This algorithm aims to optimize modularity, a measure of the quality of network  
89 division into communities, using two phases: (1) local moving of nodes and (2) aggregation of the  
90 network. In the first phase, individual nodes are moved to the community that yields the largest  
91 increase in the quality function. In the second phase, an aggregation network is obtained based on  
92 partitions, with each community in a partition becoming a node in the aggregate network. These two  
93 phases are repeated until the quality function cannot be increased further. However, the Louvain  
94 algorithm can potentially produce communities with arbitrarily poor connectivity. In the most adverse  
95 scenarios, these communities may become entirely disconnected, particularly during iterative  
96 executions of the algorithm.

97

## 98 *Leiden algorithm*

99 To address the connectivity issues of the Louvain algorithm, V. A. Traag et al. introduced the Leiden  
100 algorithm [10]. The Leiden algorithm guarantees that communities are well connected and, when  
101 applied iteratively, the algorithm converges to a partition where all subsets of all communities are  
102 locally optimally assigned. The Leiden algorithm is partly based on the smart local move algorithm,  
103 which itself can be seen as an improvement of the Louvain algorithm and takes advantage of the idea  
104 of speeding up the local moving of nodes and the idea of moving nodes to random neighbors, the  
105 Leiden algorithm considers these ideas to represent the most promising directions in which the  
106 Louvain algorithm can be improved. The Leiden algorithm consists of three phases: (1) local moving of  
107 nodes, (2) refinement of the partition, and (3) aggregation of the network based on the refined  
108 partition, using the non-refined partition to create an initial partition for the aggregate network. Thus,  
109 this algorithm optimizes a quality function to identify communities by considering the density of  
110 connections within the communities.

111

## 112 *MClust*

113 MClust [11], applied in cell clustering, identifies distinct cell groups based on observed features using  
114 Gaussian mixture models [12]. Unlike other clustering algorithms, MClust accommodates various  
115 cluster shapes, making it suitable for complex situations. It utilizes the Expectation-Maximization [13]  
116 algorithm for parameter estimation, offering robust handling of missing data and complex  
117 distributions. This model-based clustering tool is powerful in uncovering patterns within complex  
118 biological datasets, such as those from single-cell omics technologies. Initially designed for single-cell  
119 RNA sequencing data, it can also be applied to spatial transcriptomic data, its effectiveness depending  
120 on data characteristics and analysis goals.

121

## 122 *Embedding methods from the literature*

123

124 In spatial transcriptomics, where data is organized as a matrix with cells and genes, the high  
125 dimensionality (often exceeding 30,000 genes) and sparsity pose analytical challenges. Dimensionality  
126 reduction methods play key roles in addressing these issues. These techniques help distill meaningful  
127 patterns from the data, facilitating more efficient analyses.

128 The generation of embeddings, achieved through established literature methods, aims to  
129 transform the high-dimensional gene space into a more manageable form. This process enables a  
130 clearer exploration of spatial relationships, cell heterogeneity, and underlying biological processes. By  
131 leveraging validated methods from existing literature, we ensure a scientifically rigorous approach,

132 condensing rich gene expression profiles into interpretable embeddings while addressing  
133 computational complexities.

134 As mentioned previously, we performed dimensionality reduction using five different  
135 embedding methods: STAGATE [14], Principal Component Analysis (PCA) [15], GraphST [16], Cell  
136 Clustering for Spatial Transcriptomics (CCST) data [17], and STAligner [18].

137

#### 138 *STAGATE*

139 The STAGATE method [14] has been designed for spatial clustering and denoising in spatially resolved  
140 transcriptomics data. This method generates low-dimensional latent embeddings with both spatial  
141 information and gene expressions via a graph attention auto-encoder. Notably, the method adopts an  
142 attention mechanism in the middle layer of the encoder and decoder, which learns the edge weights  
143 of spatial neighbor networks and uses them to update spot representations by collectively aggregating  
144 information from their neighbors.

145

#### 146 *Principal Component Analysis*

147 PCA [15] is a statistical method for dimensionality reduction and data visualization. It is a mathematical  
148 procedure that transforms a set of correlated variables into a new set of uncorrelated variables known  
149 as principal components. The principal components are linear combinations of the original variables  
150 and are sorted based on how much they account for the variance within the data; i.e., the first principal  
151 component accounts for the highest variance. PCA finds widespread application across domains,  
152 including data analysis, machine learning, and image processing, aiming to streamline intricate  
153 datasets and uncover patterns or associations between variables.

154

#### 155 *GraphST*

156 GraphST [16] is an advanced self-supervised contrastive learning technique designed to maximize the  
157 potential of spatial transcriptomics data. Integrating graph neural networks with self-supervised  
158 contrastive learning, this method acquires spot representations that are both informative and  
159 distinctive. This is achieved by minimizing the embedding distance between spatially neighboring spots  
160 reciprocally.

161

#### 162 *Cell Clustering for Spatial Transcriptomics data*

163 CCST [17] leverages graph convolutional networks (GCNs) to integrate gene expression data and  
164 comprehensive spatial information from individual cells in spatial gene expression data. The  
165 relationships between variables are captured as a graph, with the adjacency matrix representing  
166 connections among variables and the node feature matrix reflecting variable observations. The GCN  
167 layer is strategically designed to fuse graph (in our case, spatial structure) and node features (gene  
168 expression). Initially, the data is transformed into a graph, where nodes represent cells with gene  
169 expression profiles as attributes, and edges represent neighborhood relationships between cells.  
170 Subsequently, a sequence of GCN layers is used to incorporate graph and gene expression details into  
171 cell node embedding vectors. Concurrently, the graph is perturbed to generate negative embeddings.  
172 By learning the discrimination task, the neural network model is trained to encode cell embeddings  
173 derived from spatial gene expression data, subsequently used for cell clustering.

174

#### 175 *STAligner*

176 STAligner [18] is a specialized tool for aligning and integrating spatially-resolved transcriptomics data.  
177 It begins by normalizing expression profiles for all spots and creating a spatial neighbor network based  
178 on spatial coordinates. Employing a graph attention auto-encoder neural network, STAligner extracts

179 spatially-aware embeddings and uses spot triplets to guide the alignment process, fostering similarity  
 180 among related spots and distinction among dissimilar ones across slices. The introduction of triplet  
 181 loss refines spot embeddings by minimizing the distance from the anchor to positive spots and  
 182 increasing the distance to negative spots. This iterative process optimizes triplet construction and auto-  
 183 encoder training until batch-corrected embeddings are obtained. Furthermore, STAligner's versatility  
 184 extends to integrating spatial transcriptomics datasets, facilitating alignment and concurrent  
 185 identification of spatial domains across diverse biological samples, technological platforms,  
 186 developmental stages, disease conditions, and consecutive tissue slices for 3D alignment.  
 187

## 188 Implementation

### 189 Mathematical model

190

191 Let  $C = [c_i]$  represent the set of cells  $c_i, i = 1, \dots, n$ , and the total number of cells equal  $n$ . For each  
 192 cell  $c_i, i = 1, \dots, n$ , let  $c_i^x$  and  $c_i^y$  represent its  $x$  and  $y$  coordinates, and let vector  $c_i^{emb} =$   
 193  $[c_i^{emb_1}, \dots, c_i^{emb_M}]$  represent embedding values ( $M$  is the total number of embedding values).  
 194 Furthermore, let the distance function  $D: C \times C \rightarrow \mathcal{R}^+$  be defined as a measure of the similarity  
 195 between the cells. In our model, for two cells  $c_i$  and  $c_j$ , the distance  $D$  was calculated as follows:  $D =$   
 196  $\alpha D_{gene} + (1 - \alpha)D_{coord}$ , where  $\alpha$  is the input parameter,  $D_{gene}$  is the cosine similarity between cell  
 197 embeddings, and  $D_{coord}$  is the Euclidian distance between cell coordinates:

198

$$D_{gene}(c_i, c_j) = \text{cosine}(c_i, c_j),$$

199

$$D_{coord}(c_i, c_j) = \sqrt{(c_i^x - c_j^x)^2 + (c_i^y - c_j^y)^2}.$$

200 In our model, we chose  $K$  different cells from the set of cells  $C$  to represent clusters and called these  
 201 cells *centroids*. Therefore, let the binary variables  $x_{ij} (i, j = 1, \dots, n)$  and  $y_i$  be defined in the following  
 202 way:

203

$$x_{ij} = \begin{cases} 1, & \text{if cell } c_i \text{ belongs to the cluster represented by centroid } c_j \\ 0, & \text{otherwise} \end{cases}$$

204

$$y_i = \begin{cases} 1, & \text{if cell } c_i \text{ represents the centroid} \\ 0, & \text{otherwise} \end{cases}$$

205 The Integer Linear Programming formulation of the clustering problem can be described as follows:

206

$$\min \sum_{i=1}^n \sum_{j=1}^n x_{ij} D(c_i, c_j) \quad (1)$$

207 subject to these constraints:

208

$$\sum_{i=1}^n x_{ij} = 1, \quad 1 \leq j \leq n, \quad (2)$$

209

$$x_{ij} \leq y_j, \quad 1 \leq i \leq n, \quad 1 \leq j \leq n, \quad (3)$$

210

$$\sum_{i=1}^n y_i = K, \quad (4)$$

211

$$x_{ij}, y_j \in \{0, 1\}, \quad 1 \leq i \leq n, \quad 1 \leq j \leq n. \quad (5)$$

212 The objective function (1) represents the sum of distances from each cell to its most similar cluster  
 213 representative. This function should be minimized. Equation (2) indicates that each cell is assigned to  
 214 only one cluster. Before assigning a cell to a cluster, the cluster needs to be defined (3). The total  
 215 number of clusters is equal to  $K$  (4). All variables are constrained to be binary (5).

216 The model described with equations (1)-(5) is based on the  $p$ -median classification and is  
 217 presented in a similar form by Davidović et al. [19].  
 218

## 219 Variable Neighborhood Search Method

220

221 The VNS method is a well-known metaheuristic method. It starts from one point in the search  
222 space, explores its neighborhoods, and repeats the process until a better solution or stopping criteria  
223 are reached. This method was proposed for the first time by Mladenović [20] and later elaborated by  
224 Mladenović and Hansen [21] and Hansen and Mladenović [22].

225 Before we introduce the VNS method, let us define the set  $N_k(X)$ ,  $k = k_{\{min\}}, \dots, k_{max}$  as the  
226 set of all vectors  $X'$  that have a difference of the  $k^{th}$  order from the solution  $X$ , and call that set  $k^{th}$   
227 Neighborhood to the solution  $X$ .

228 The VNS-based heuristic can be defined in a way that it starts from the initial feasible solution  
229  $X$ , shakes it by creating another solution  $X' \in N_k(X)$ , and then applies a local search method to create  
230 a better feasible solution  $X''$ . If the feasible solution  $X''$  obtained by the local search procedure is not  
231 better than the current incumbent  $X$  ( $F(X'') \geq F^*$ ), the VNS algorithm repeats the procedure of  
232 shaking in the neighborhood  $N_{k+k_{step}}$  (i.e.,  $k$  is incremented by  $k_{step}$ ) and local searches within it. It  
233 repeats this passage until  $k$  reaches its maximum  $k_{max}$ . Otherwise, if  $F(X'') < F^*$ ,  $F^*$  becomes  
234  $F(X'')$  and  $k$  becomes  $k_{min}$ . The procedure of changing the neighborhood enables the VNS algorithm  
235 to get out from the local minima. The process is repeated until a certain number of iterations or other  
236 stop criteria are reached.

237 Pseudo-code for the basic VNS algorithm is presented as Algorithm 1. Implementations of the  
238 functions *InitialSolution()*, *Shake()*, *LocalSearch()*, and *StoppingCondition()* defined for our clustering  
239 problem are described in the following subsection.

240

---

### Algorithm 1 (Basic) Variable Neighborhood Search Method

---

```
1:  $X^* \leftarrow InitialSolution()$   
2:  $F^* \leftarrow F(X^*)$   
3: while StoppingCondition() do  
4:    $k \leftarrow k_{min}$   
5:   while  $k \leq k_{max}$  do  
6:      $X \leftarrow X^*$   
7:      $X' \leftarrow Shake(X, k)$   
8:      $X'' \leftarrow LocalSearch(X')$   
9:     if  $F(X'') < F^*$  then  
10:       $X^* \leftarrow X''$   
11:       $F^* \leftarrow F(X^*)$   
12:       $k \leftarrow k_{min}$   
13:     else  
14:       $k \leftarrow k + k_{step}$   
15:     end if  
16:   end while  
17: end while
```

---

241

242

## 243 VNS for the cell clustering problem

244

245 With respect to the problem's definition, let us assume that all cells can be represented by numbers  
246 from 1 to  $n$ . Specifically, cells can be represented by the set  $C = [c_i]$ ,  $n = |C|$ , and that for each cell  
247  $c_i$  there are two types of data: the  $x$  and  $y$  coordinates of the cell ( $c_i^x$  and  $c_i^y$ ) and the embedding  
248 values (vector  $emb_i$ ). In our representation, the solution vector  $Y = [y_1, \dots, y_K]$  contains indexes of  $K$   
249 cells chosen as cluster representatives. Also, cell  $y_i$  is a centroid of the  $i$ -th cluster. From the centroid  
250 solution vector  $Y$  we obtain vector  $X = [x_i]$  of size  $n$  in the following way:  $x_i$ ,  $i = 1, \dots, n$ , represents  
251 the closest centroid from the  $Y$  vector to the  $i$ -th cell. Our representation satisfies all conditions  
252 described by equations (2) - (5). Using this representation, our goal was to minimize the value of the  
253 function  $F: C \times C \rightarrow \mathcal{R}^+$ , where  $F$  is defined as  $F(X) = \sum_{i=1}^n (\alpha D_{gene}(i, x_i) + (1 -$   
254  $\alpha) D_{coord}(i, x_i))$ .

255 The function *InitialSolution()* randomly chooses  $K$  mutually different numbers from the set of  
256 numbers  $\{1, \dots, n\}$  and returns them as a  $K$ -dimensional vector  $Y$ . For every solution vector  $Y$ , vector  
257  $X$  is obtained in the following way: for each cell  $i$ , the distance  $D$  between the cell  $i$  and all centroids  
258  $y_j$  from the vector  $Y$  is calculated; next,  $x_i$  is set equal to the  $y_j$  for which the distance  $D$  is minimal.  
259 That is, whenever the vector  $Y$  is changed, vector  $X$  is also updated. Also, to avoid repeated  
260 calculations, the distance  $D$  between all cells is calculated and saved as a *distance* matrix.

261 The *Shake()* function takes two inputs: the incumbent  $Y$  and the size  $k$  of the neighborhood  
262 that needs to be explored. As a result, the *Shake()* function randomly chooses  $k$  elements from the  
263 vector  $Y$  and replaces them with  $k$  randomly chosen elements from the set  $\{1, \dots, n\}$  that are different  
264 from all elements from the current  $Y$ . This means that when some elements are changed, all elements  
265 in vector  $Y$  will still be mutually different. In other words, the *Shake()* function chooses a vector  $Y'$   
266 from  $N_k(Y)$ .

267 The *LocalSearch()* function takes vector  $Y'$ , the distance matrix *distance*, and the parameters  
268  $m$  and  $p$  as inputs. In our implementation, we used *the first improvement strategy*. Based on the value  
269 of the parameter  $m$ , for each element of the vector  $Y'$ , the *LocalSearch()* function first chooses a  
270 random integer number  $ind \in [0, m]$ ; next, based on the  $ind$  value, keeps the observed element of  
271 the vector  $Y'$  as it is ( $ind == 0$ ) or replace it with the new one ( $ind > 0$ ). For  $ind \geq 2$ , the observed  
272 element is replaced with one of the candidates from the set of candidates that are created within the  
273 *LocalSearch()* function (the *LocalSearch()* function searches for  $ind$  candidates for which the *distance*  
274 value from the observed candidate is the smallest, sorts the list, excludes all candidates that are  
275 already present in the vector  $Y'$ , and then chooses one candidate for the replacement). Please note  
276 that the smallest *distance* value between the observed candidate and itself will be zero, so the  
277 condition  $ind > 1$  is necessary. In case  $ind == 1$ ,  $ind$  will be chosen again until its value is not equal  
278 to 1. Additionally, if the candidate list is empty after excluding all elements that already exist in the  
279 vector  $Y'$ , a random candidate will be chosen from the set  $\{1, \dots, n\} \setminus \{y_1, \dots, y_K\}$ .

280 Finally, after the procedure of replacing or keeping elements from the vector  $Y'$  is finished, i.e., a new  
281 vector  $Y''$  is obtained, the *LocalSearch()* function calculates  $F(Y'')$  and, if  $F(Y'') < F^*$ , the first  
282 improvement has been made, and the function returns the vector  $Y''$  as the output or repeats the  
283 whole process. The process of examining elements of the vector  $Y'$  and replacing them with new  
284 values is repeated only if no improvement is made, but not more than  $p$  times. In case no improvement  
285 is made and the process has been repeated  $p$  times, the vector  $Y'' = Y'$  will be returned as the output  
286 of this function.



287 In other words, the *LocalSearch()* function examines elements in the close neighborhood of  
288 the observed vector  $Y'$  by creating a new vector  $Y''$ , calculates the function value  $F(Y'')$  and, if the  
289 function value is less than the currently best value  $F^*$ , returns that vector. Otherwise, it will continue  
290 the process of examining elements of the vector  $Y'$  but not more than  $p$  times.

291 Usually, the *StoppingCondition()* function checks if the maximal number of iterations  
292 ( $max_{iter}$ ) or the maximal running time ( $t_{max}$ ) have been reached. In our code, the *StoppingCondition()*  
293 function checks only if the maximal number of iterations has been reached and, if the answer is *true*,  
294 returns the best solution found as the result of the VNS procedure. If the maximal number of iterations  
295 has not been reached, the VNS procedure continues its search.

296

## 297 Data Description

298

299 We assessed the performance of the clustering methods through quantitative evaluation, employing  
300 datasets sourced from two distinct spatially resolved transcriptomic technologies: Stereo-seq [23] and  
301 10x Visium [24].

302 From Stereo-seq technology, two datasets were used for testing: a large dataset of a field  
303 mouse brain hemisphere (**SS200000128TR E2 benchmark**) and another from the dorsal midbrain  
304 (**Forebrain**). The large field mouse brain contains more than 38,000 cells and more than 20,000 genes  
305 and can be downloaded from [25], while Forebrain contains more than 18,000 cells and more than  
306 23,000 genes and can be downloaded from [26]. Please note that Forebrain contains the whole dorsal  
307 midbrain. In our study, we used manual lasso to separate a part of this dataset and called that part  
308 **Forebrain**. Both datasets are composed of only one slice.

309 In order to evaluate the performance of the presented VNS method on multi-slice datasets,  
310 we used a 10x Visium dataset containing spatial expressions of 12 human-layered dorsolateral  
311 prefrontal cortex (DLPFC) sections. Since these 12 sections are from three different human donors,  
312 they were used as multi-section (4-layers) datasets in our study. All layers of the DLPFC sections were  
313 manually annotated by Maynard et al. [24] and can be downloaded from [27]. Viewing them as the  
314 ground truth, we compared the clustering accuracy of the VNS method with other clustering methods  
315 using only embedding obtained by the vertical spatial transcriptomic integration provided by  
316 STAGATE.

## 317 Analysis

### 318 Input parameters

319

320 Testing was conducted on the AWS instance **m6a.48xlarge** under the Linux operative system.

321 Input parameters for our algorithm are the number of clusters ( $K$ ), the percentage of the  
322 influence of the embedding values ( $\alpha$ ), the maximal number of neighborhoods that should be  
323 searched ( $k_{max}$ ), the maximal number of iterations ( $max_{iter}$ ), and the *local search* parameters  $m$  and  
324  $p$ . The minimal ( $k_{min}$ ) number of neighborhoods and step ( $k_{step}$ ) are set to 1 by default.

325 The input parameters used for testing are  $\alpha \in \{1, 0.95\}$  ( $\alpha = 1$  means that no additional  
326 spatial information is included, while  $\alpha = 0.95$  means that 5% of spatial information is used for  
327 calculating the distance between the cells),  $k_{max} \in \{10, 15, 20, 25, 30\}$ ,  $m \in \{10, 12, 15, 20, 30\}$ , and  
328  $p \in \{10, 12, 15, 20\}$ .

329



## 330 Evaluation method

331

332 We used the Adjusted Rand Index (ARI) [28] to evaluate the results and compare them with each other.  
333 ARI is a measure used to evaluate the performance and similarity between two clustering algorithms.  
334 It quantifies the agreement between the true and predicted clustering, adjusting for the amount of  
335 agreement that could occur by chance. ARI values range from -1 to 1: where 1 indicates the perfect  
336 agreement, 0 indicates agreement expected by chance, and negative values suggest less agreement  
337 than expected by chance.

338

## 339 Results of the VNS method across various scenarios with single-slice datasets

340

341 Due to the sparsity of the gene expression matrix and to ensure a fair comparison, embeddings were  
342 obtained using various methods from the literature (PCA, STAGATE, GraphST, and CCST) for both  
343 Stereo-seq datasets. Moreover, all methods create embedding that significantly reduces the number  
344 of genes to a much smaller set of features. For instance, the CCST method reduced the number of  
345 genes from the Forebrain dataset to 128 features, STAGATE to 64 features, PCA to 50 features, and  
346 GraphST to 20 features. For the E2 dataset, all parameters were the same except for STAGATE, where  
347 the number of features was lowered to 30. Hence, the input data depend on the number of cells and  
348 the number of obtained features (embeddings). The standard clustering methods from the literature  
349 ( $k$ -Means, MClust, Louvain, and Leiden) and the proposed VNS method for cell clustering were applied  
350 to the generated embeddings. The results of the testing are presented in Tables 1 and 2.

351

352 The goal of the VNS method was to find the solution with the smallest cost function, and we  
353 show these results in Table 1. Table 1 shows results obtained by the VNS method only and is organized  
354 as follows: the first column presents the name of the embeddings used as the input to the VNS method,  
355 while the following four columns ( $f_{VNS}$ ,  $t_{VNS}$ ,  $err$ , and  $\sigma$ ) show the smallest cost function value, the  
356 corresponding running time, and the statistical analysis of all solutions obtained by VNS when  
357 comparing to the presented cost function value in that order. In other words, due to the stochastic  
358 nature of the metaheuristic, the VNS algorithm was run 20 times (for 20 different seeds) for each  
359 embedding, and information regarding the best solution value obtained in these 20 runs is provided  
360 in these four columns ( $f_{VNS}$ ,  $t_{VNS}$ ,  $err$ , and  $\sigma$ ). More precisely,  $f_{VNS}$  presents the minimal cost  
361 function value obtained after these 20 runs;  $t_{VNS}$  is the corresponding running time for the presented  
362 solution value;  $err$  and  $\sigma$  contain additional information on the quality of the solution:  $err$  is the  
363 average relative error of found solution from the presented one and is calculated as  $err =$   
364  $\frac{1}{20} \sum_{i=1}^{20} err_i$ , where  $err_i = |VNS_i - f_{VNS}| / |VNS_i|$ , where  $VNS_i$  is the VNS solution obtained in the  
365  $i^{th}$  run (seed). The value  $\sigma$  is the standard deviation of  $err$  and is calculated by  $\sigma =$   
366  $\sqrt{\frac{1}{20} \sum_{i=1}^{20} (err_i - err)^2}$ . For each embedding method, the results obtained by VNS are presented in  
367 separate rows.

367

368 The results presented in Table 2 are organized into three groups. Similar to Table 1, the first  
369 column (first group) presents the name of the method used for creating the embedding. The next ten  
370 rows present the results for each clustering method separately; for each method, we provide the ARI  
371 score ( $ARI$ ) and the running time ( $t$ ) in seconds. The  $ARI$  and  $t$  values under the VNS columns stand  
372 for the best found  $ARI$  score obtained for all testing combinations and the corresponding running  
373 time. The highest  $ARI$  score achieved for some datasets among all clustering methods is highlighted  
374 in bold, while the second-best  $ARI$  score is highlighted by an asterisk (\*).

374 In both tables, the first set of results corresponds to the E2 dataset, and the next corresponds  
 375 to the Forebrain dataset. The E2 dataset results are visualized in Figure 1, while the Forebrain dataset  
 376 results are visualized in Figure 2.

377  
 378 **Table 1.** VNS solution for single-slice datasets. Values in columns  $f_{VNS}$ ,  $t_{VNS}$ ,  $err$  and  $\sigma$  are  
 379 obtained as explained in the Analysis section.

380

Embedding	$f_{VNS}$	$t_{VNS}$ (s)	$err$	$\sigma$
E2				
CCST	1,019.7419	48.8355	0.1626	0.0476
STAGATE	2,706.7446	110.258	0.1196	0.0415
PCA	9,550.0142	79.1977	0.0320	0.0118
GraphST	10,083.5379	64.95	0.0197	0.0059
Forebrain				
CCST	427.8511	47.8054	0.1579	0.0439
STAGATE	543.0947	52.7096	0.0925	0.0347
PCA	3,541.7886	50.1935	0.0214	0.0073
GraphST	2,209.235	92.0103	0.0473	0.0140

381  
 382 **Table 2.** Clustering method comparison for single-slice datasets. The highest *ARI* score  
 383 achieved for some datasets among all clustering methods is highlighted in bold, while the second-best  
 384 *ARI* score is highlighted by an asterisk (\*).  
 385

Embeddings	Leiden		Louvain		<i>k</i> -Means		MClust		VNS	
	<i>ARI</i>	<i>t</i> (s)	<i>ARI</i>	<i>t</i> (s)	<i>ARI</i>	<i>t</i> (s)	<i>ARI</i>	<i>t</i> (s)	<i>ARI</i>	<i>t</i> (s)
E2										
CCST	0.1553	29.1638	0.1518	5.7702	0.1962*	15.3243	0.1401	4,799.5287	<b>0.2224</b>	47.5667
STAGATE	0.1951	7.5198	0.2176	6.3803	<b>0.2907</b>	2.62854	0.2052	516.8929	0.2890*	59.7737
PCA	0.0001	6.8347	0.1316	9.9780	0.2072*	12.0037	0.2024	1,128.1911	<b>0.2907</b>	235.465
GraphST	<b>0.0841</b>	14.8255	0.0697*	13.0344	0.0492	4.2599	0.0635	533.1441	0.0636	47.5184
Forebrain										
CCST	0.0925	25.7164	0.0961*	2.5659	0.1093	8.7788	0.0821	1,330.3455	<b>0.1263</b>	18.6987
STAGATE	0.1753	3.6952	0.1676	3.6263	0.1775*	6.0085	0.1718	269.9742	<b>0.2342</b>	24.6907
PCA	0.1659	4.4805	0.1674*	3.7720	<b>0.1717</b>	6.4302	0.1025	147.4443	0.1568	45.2866
GraphST	0.1738	3.8813	0.1847*	4.6558	0.1833	1.8972	0.1709	73.0143	<b>0.2104</b>	9.2064

386  
 387  
 388 VNS clustering achieves better results than other tested methods using the E2 dataset  
 389

390 From the first part of the results shown in Table 1, we can conclude that, using PCA embedding in all  
 391 20 runs, the values of the cost function are very close to the lowest cost function value ( $err < 3.5$ ,  
 392  $\sigma < 1.5\%$ ). Using STAGATE, we have some differences, although  $\sigma$  is still below 5% implying that the

393 VNS method is stable with both embeddings. The results of VNS clustering when the smallest cost  
394 function values are reached are visualized in Figure 1a, while the results with the best ARI score  
395 achieved by all clustering methods are shown in Figure 1b.

396

397 VNS methods outperform other methods when clustering cells from the Forebrain dataset

398

399 By examining values from the *err* and  $\sigma$  columns in Table 1 for the Forebrain dataset, it can be easily  
400 seen that differences between the results obtained in 20 runs are very small. In fact, the difference  
401 between the best-found solution (the solution with the minimal cost function value) and the other 19  
402 solutions is less than 5% (the average relative error  $\sigma$  is less than 5%). This result means that the  
403 solutions found in all 20 runs were very close to the smallest one. Also, from the results in the column  
404  $t_{VNS}$ , we can observe a running was less than 1 minute for three different embedding types and less  
405 than 2 minutes for one embedding type.

406 Moreover, from the results presented in Table 2 for the Forebrain dataset, we can see that, in  
407 the majority of cases, VNS had the highest ARI score compared to the other methods (for three types  
408 of embedding, the VNS ARI score was the highest). Also, the running time was less than 1 minute for  
409 each type of embedding. The only embedding for which the VNS did not find a solution with the best  
410 ARI score was the PCA one, and for this embedding, the best ARI score was obtained by the *k*-Means  
411 method.

412 By analyzing the results in Tables 1 and 2, we conclude that the VNS method achieves the best  
413 ARI score with the STAGATE embedding, and that in all 20 runs all solutions were close to the one  
414 with the lowest cost function ( $err < 1\%$ ). The results obtained with the minimal cost function and  
415 the maximal ARI score are visualized in Figure 2.

416

417

418

419 VNS demonstrates a superior performance on multi-slice datasets

420

421 Next, we compared the clustering accuracy of the VNS method with other clustering methods by using  
422 embeddings obtained by the STAligner method only. Compared to other embedding methods used for  
423 single-slice datasets, it is worth mentioning that STAligner reduces the number of genes to 30 features.  
424 The results of this comparison are presented in Tables 3 and 4. Table 3 is organized similarly to Table  
425 1. The only difference is in the first column, which, in this case, is called Slice name. Since DLPFC  
426 datasets are 4-layered slices, this column contains the names of the first and the last slices in this  
427 particular dataset. Other slices imply. Thus, each row represents the results for one separate DLPFC  
428 dataset.

429 Table 4 is organized similarly to Table 2; however, the column Embeddings is replaced by the  
430 column Slice name, and the names of the first and the last slices from particular multi-slice datasets  
431 are presented. Other slices imply. The results for each dataset are presented in separate rows, as in  
432 Table 3. The results from Table 3 are visualized in Figure 3.

433 As we see from the columns *err* and  $\sigma$  in Table 3, in all 20 runs, the VNS method obtained  
434 results similar to the ones with the smallest cost function ( $err < 5.8\%$ ,  $\sigma < 2.5\%$ ). Again, these results  
435 imply that the method is stable even for multi-slice datasets. The fact that results from the columns  
436  $t_{VNS}$  are smaller than 5 implies that this method can obtain results for four slices of these types of  
437 datasets in less than 5 seconds.

438 From the results presented in Table 4, it can be concluded that the method proposed in this  
 439 paper outperforms other clustering methods in all aspects. Specifically, for each of the datasets we  
 440 tested, *ARI* score was the highest and the running time was the lowest when the VNS method was  
 441 used.

442

443 **Table 3.** VNS solution for multi-slice datasets.

Slice name	$f_{VNS}$	$t_{VNS}$	$err$	$\sigma$
151507_151510	890.7088	4.2262	0.0884	0.0390
151669_151672	755.7133	2.8674	0.0866	0.0273
151673_151676	513.8781	1.1983	0.0923	0.0396

444

445 **Table 4.** Clustering method comparison for multi-slice datasets. The highest *ARI* score achieved for  
 446 some datasets among all clustering methods is highlighted in bold, while the second-best *ARI* score is  
 447 highlighted by an asterisk (\*).

Slice name	Leiden		Louvain		<i>k</i> -Means		MClust		VNS	
	<i>ARI</i>	<i>t</i> (s)	<i>ARI</i>	<i>t</i> (s)	<i>ARI</i>	<i>t</i> (s)	<i>ARI</i>	<i>t</i> (s)	<i>ARI</i>	<i>t</i> (s)
151507_151510	0.3440	27.3778	0.4293*	4.0119	0.3061	2.1001	0.3489	62.5176	<b>0.4887</b>	2.1094
151669_151672	0.4084	26.9197	0.4985*	2.9611	0.2213	1.6839	0.4633	39.1007	<b>0.6156</b>	1.3014
151673_151676	0.4370	25.1056	0.4754*	2.6766	0.3299	1.4413	0.4316	49.1890	<b>0.5016</b>	0.8573

448

## 449 Discussion and Conclusion

450

451 Here, we introduced a novel approach suitable for clustering both single- and multi-slice spatial  
 452 transcriptomics datasets. This is the first application of a metaheuristic method, called the VNS, to the  
 453 clustering of spatial transcriptomic data. The essence of the VNS implementation presented in this  
 454 study is the utilization of a combinatorial/mathematical optimization algorithm; in this instance, a  
 455 metaheuristic approach. These methods are strategically designed to deliver sufficiently optimal  
 456 solutions to optimization and machine learning challenges while minimizing computational resources.  
 457 This approach is intended to offer a robust and computationally efficient solution for cell clustering in  
 458 spatial transcriptomics.

459 Our analysis demonstrated that the performance of clustering methods is significantly influenced by  
 460 the choice of embeddings and the way they were generated. Notably, the VNS approach combined  
 461 with PCA embeddings yields results that closely align with the ground truth, as illustrated in Figure 2b.  
 462 When benchmarked against existing techniques, our method consistently outperforms in terms of  
 463 efficiency and *ARI* scores. The algorithm's speed and stability are commendable, and its flexibility is  
 464 evidenced by a comprehensive set of parameters that can be tailored to meet diverse user  
 465 requirements. Future research will extend the method's application to time-series datasets and  
 466 explore additional VNS modifications and embedding techniques to enhance its utility.

467

## 468 Availability of source code and requirements:

469

- 470 • Project name: VNS

- 471 • Project home page: <https://github.com/STOmics/VNS/tree/main>
- 472 • Operating system(s): Linux
- 473 • Programming language: Python
- 474 • License: MIT
- 475 • RRID:
- 476

## 477 Data availability

478

479 From Stereo-seq technology, two datasets were used:

480 (1) a large dataset of a field mouse brain hemisphere (**SS200000128TR E2 benchmark**), which can be  
481 downloaded from Zenodo [25]

482 (2) **Forebrain**, which can be downloaded from the CNGB MOSTA database  
483 <https://db.cngb.org/stomics/mosta/download/>.

484 Additional data is also available in GigaDB [29]. We used only one part of Forebrain, which was  
485 extracted using a manual lasso.

486

## 487 Declarations

488

### 489 Abbreviations

490 ARI, Adjusted Rand Index; CCST, Clustering for Spatial Transcriptomics; DLPFC, dorsolateral prefrontal  
491 cortex; GCN, graph convolutional network; PCA, Principal Component Analysis; VNS, Variable  
492 Neighborhood Search.

493

### 494 Consent for publication

495 Not applicable.

496

### 497 Competing Interests

498 The author(s) declare that they have no competing interests.

499

### 500 Ethics approval and consent to participate

501 The authors declare that ethical approval was not required for this type of research.

502

### 503 Funding

504 This work was supported by the National Key R&D Program of China (2022YFC3400400).

505

### 506 Author's Contributions

507 AD and MI provided the idea of the solution, implementation, testing, and manuscript. JL and SF  
508 supervised the whole process. CL created embeddings for both datasets for testing.

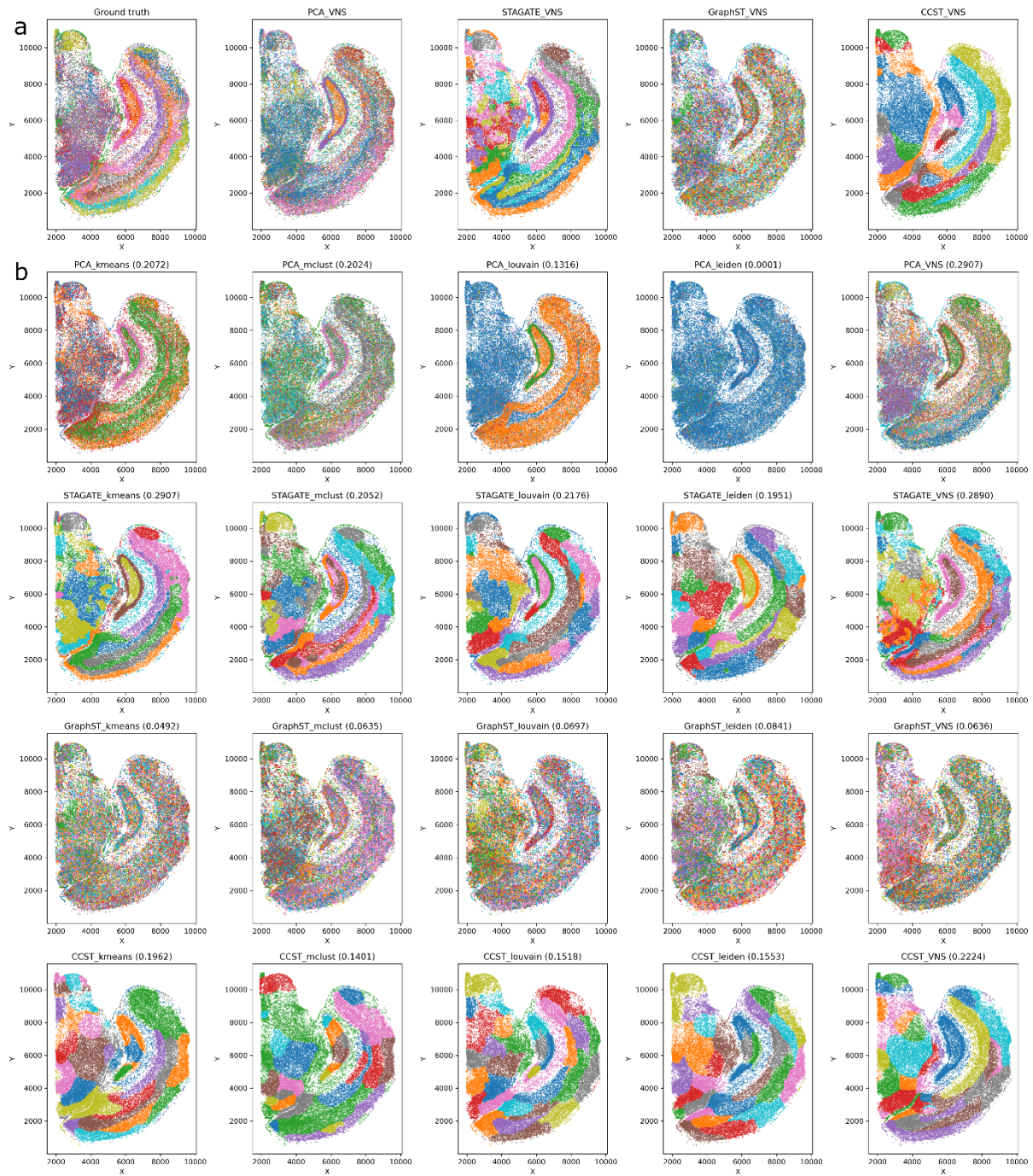
509

### 510 Acknowledgements

511 We acknowledge the CNGB Nucleotide Sequence Archive (CNSA) of China National GeneBank  
512 DataBase (CNGBdb) for maintaining the MOSTA database.

513

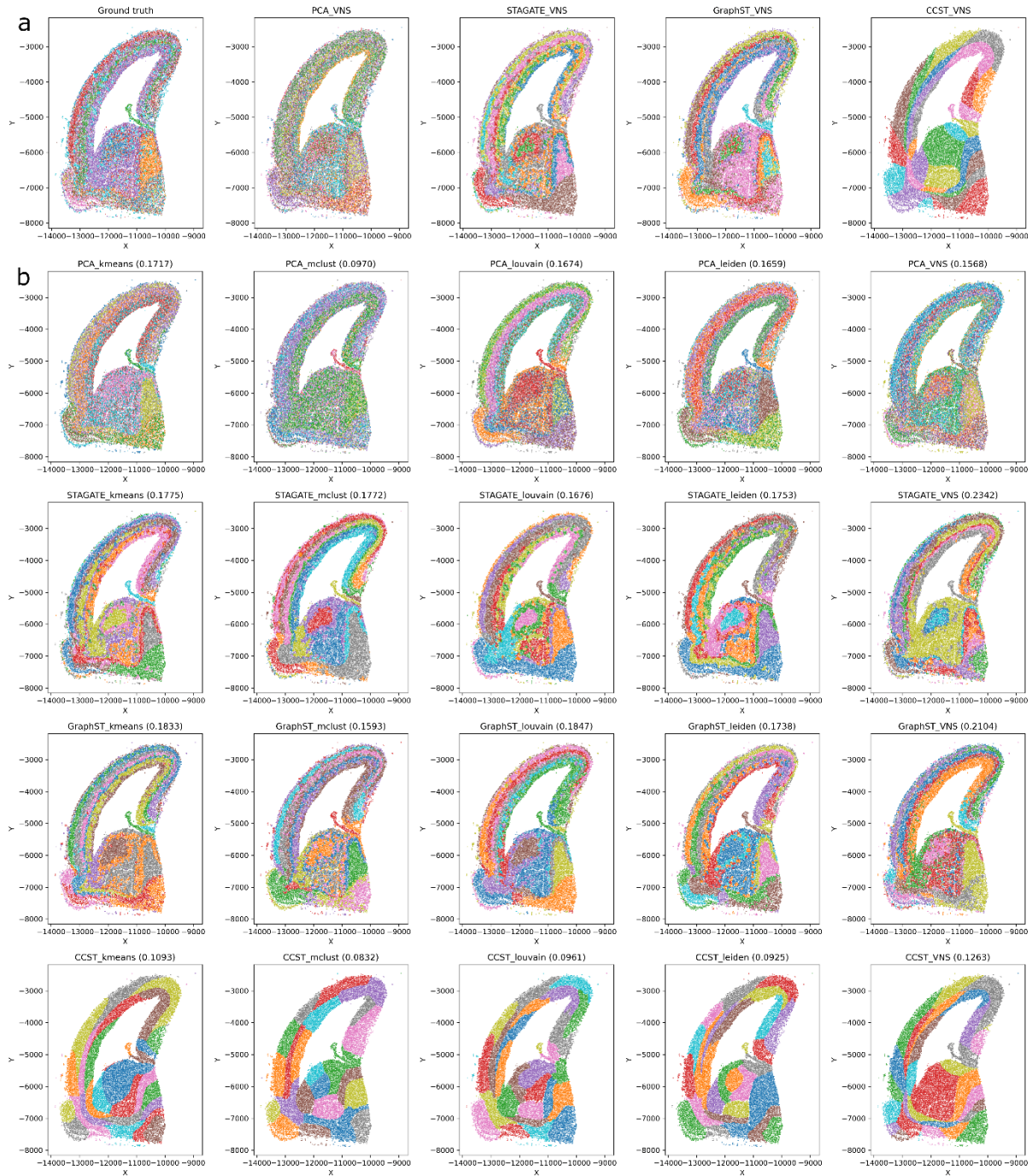




514  
515

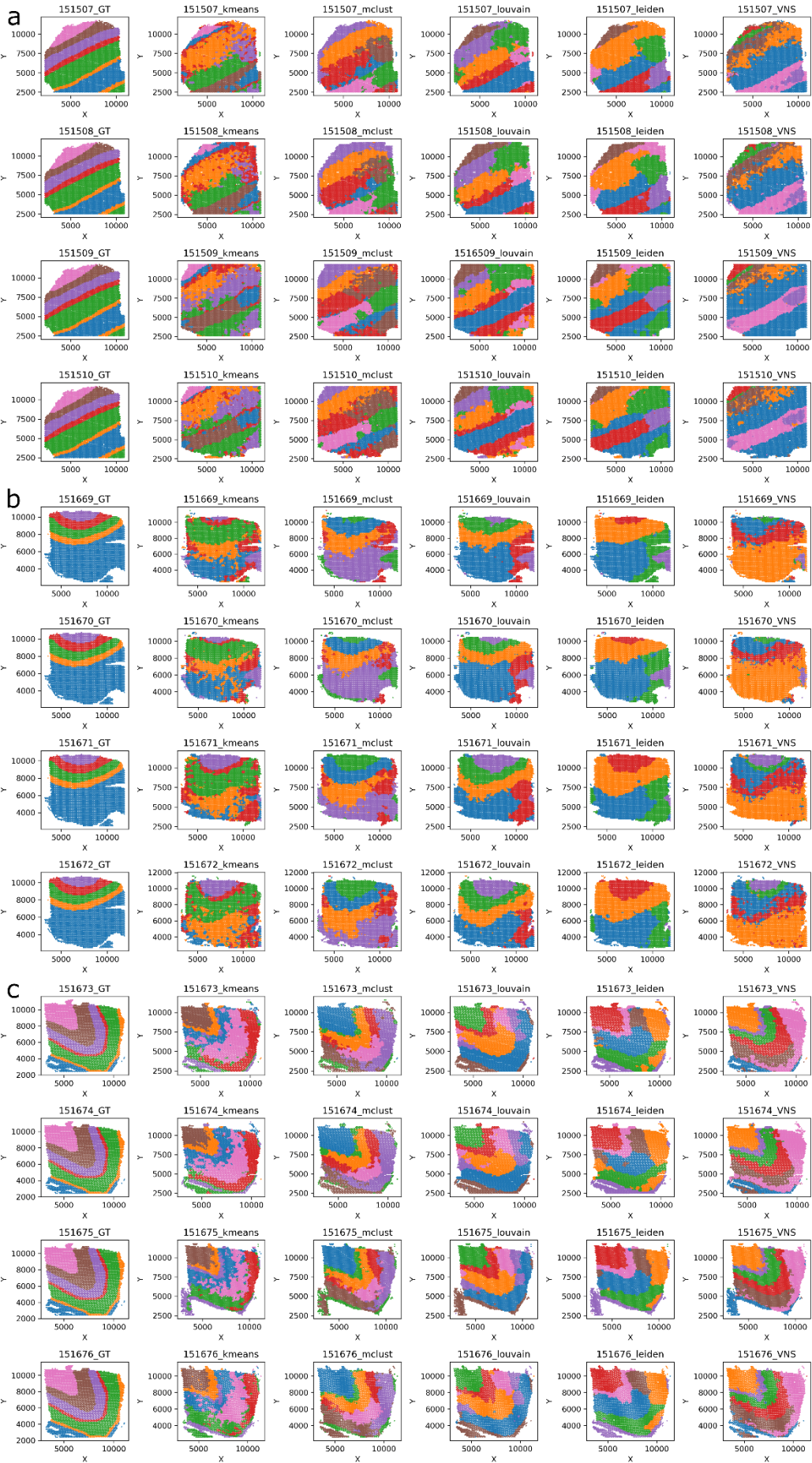
516 **Figure 1.** (a) Results of the VNS clustering on the E2 dataset. The first figure on the left presents the  
 517 ground truth data. These results were obtained using the VNS method with PCA, STAGATE, GraphST,  
 518 and CCST embeddings. (b) Clustering results for the E2 dataset. Each row presents the clustering  
 519 results obtained by  $k$ -Means, MClust, Louvain, Leiden, and VNS over a certain embedding method.  
 520 Therefore, the first row presents the results obtained by all clustering methods when using PCA  
 521 embedding. The next three rows used STAGATE, GraphST, and CCST embeddings.





522  
523

524 **Figure 2.** (a) Results of the VNS clustering on the Forebrain dataset. The first figure on the left  
 525 presents the ground truth data. These results were obtained using the VNS method with PCA,  
 526 STAGATE, GraphST, and CCST embeddings. (b) Clustering results for the Forebrain dataset. Each row  
 527 presents the clustering results obtained by  $k$ -Means, MClust, Louvain, Leiden, and VNS, over a  
 528 certain embedding method. Therefore, the first row presents the results obtained by all clustering  
 529 methods when using PCA embedding. The next three rows used STAGATE, GraphST, and CCST  
 530 embeddings.



532 **Figure 3.** The clustering results on the DLPFC datasets 151507-151510, 151669-151672, and 151673-  
533 151676 are presented in panels (a), (b), and (c), respectively. The first column shows the ground truth  
534 data, while the subsequent columns display the results obtained using *k*-Means, MClust, Louvain,  
535 Leiden, and the VNS method with STAligner embeddings.  
536

## 537 References

538

- 539 1. Giladi, A., Amit, I. Single-cell genomics: a stepping stone for future immunology  
540 discoveries. *Cell*, 2018, 172.1: 14-21.
- 541 2. Trapnell, C. et al. The dynamics and regulators of cell fate decisions are revealed by pseudo  
542 temporal ordering of single cells. *Nature biotechnology*, 2014, 32.4: 381-386.
- 543 3. Stuart, T. et al. Comprehensive integration of single-cell data. *Cell*, 2019, 177.7: 1888-1902.  
544 e21.
- 545 4. Satija, R. et al. Spatial reconstruction of single-cell gene expression data. *Nature*  
546 *biotechnology*, 2015, 33.5: 495-502.
- 547 5. Vickovic, S. et al. High-definition spatial transcriptomics for in situ tissue profiling. *Nature*  
548 *methods*, 2019, 16.10: 987-990.
- 549 6. Williams C.G., Lee H.J., Asatsuma T., Vento-Tormo R., Haque A. An introduction to spatial  
550 transcriptomics for biomedical research. *Genome Medicine* 2022;14(1):1–18.
- 551 7. Hansen, P., Mladenović, N., Brimberg, J., Pérez, J.A.M. (2010). Variable Neighborhood  
552 Search. In: Gendreau, M., Potvin, JY. (eds) Handbook of Metaheuristics. International Series  
553 in Operations Research & Management Science, vol 146. Springer, Boston, MA.  
554 [https://doi.org/10.1007/978-1-4419-1665-5\\_3](https://doi.org/10.1007/978-1-4419-1665-5_3)
- 555 8. MacQueen J, et al. Some methods for classification and analysis of multivariate observations.  
556 In: Proceedings of the fifth Berkeley symposium on mathematical statistics and probability,  
557 vol. 1 Oakland, CA, USA; 1967. p. 281–297.
- 558 9. Blondel V.D., Guillaume J.L., Lambiotte R., Lefebvre E. Fast unfolding of communities in large  
559 networks. *Journal of statistical mechanics: theory and experiment* 2008;2008(10): P10008.
- 560 10. Traag V.A., Waltman L., Van Eck N.J. From Louvain to Leiden: guaranteeing well-connected  
561 communities. *Scientific reports* 2019;9(1):5233.
- 562 11. Fraley C., Raftery A. MCLUST: Software for model-based cluster and discriminant analysis.  
563 Department of Statistics, University of Washington: Technical Report 1998; 342:1312.
- 564 12. Reynolds D.A., et al. Gaussian mixture models. *Encyclopaedia of biometrics* 2009; 741(659-  
565 663).
- 566 13. Moon TK. The expectation-maximization algorithm. *IEEE Signal processing magazine*  
567 1996;13(6):47–60.
- 568 14. Dong K., Zhang S. Deciphering spatial domains from spatially resolved transcriptomics with  
569 an adaptive graph attention autoencoder. *Nature communications* 2022;13(1):1739.
- 570 15. Karamizadeh S., Abdullah S.M., Manaf A.A., Zamani M., Hooman A. An overview of principal  
571 component analysis. *Journal of Signal and Information Processing* 2013;4(3B):173.
- 572 16. Long Y, Ang KS, Li M, Chong KKL, Sethi R, Zhong C, et al. Spatially informed clustering,  
573 integration, and deconvolution of spatial transcriptomics with GraphST. *Nature*  
574 *Communications* 2023;14(1):1155.
- 575 17. Li J, Chen S, Pan X, Yuan Y, Shen HB. Cell clustering for spatial transcriptomics data with  
576 graph neural networks. *Nature Computational Science* 2022;2(6):399–408.
- 577 18. Zhou, X., Kangning D., and Shihua Z. "Integrating spatial transcriptomics data across different  
578 conditions, technologies and developmental stages." *Nature Computational Science* (2023):  
579 1-13.



580 19. Davidovic T, Glišovic N, Raškovic M. Bee colony optimization for clustering incomplete data.  
581 In: The 7th International Conference on Optimization Problems and Their Applications,  
582 OPTA-2018; 2018. <https://ceur-ws.org/Vol-2098/paper8.pdf>  
583 20. Mladenovic N. A variable neighborhood algorithm-a new metaheuristic for combinatorial  
584 optimization. In: papers presented at Optimization Days, vol. 12; 1995.  
585 21. Mladenovic N, Hansen P, Variable neighbourhood search, computer and operations  
586 research. Computers & Operations Research 1997; 24(11) p1097-1100  
587 [https://doi.org/10.1016/S0305-0548\(97\)00031-2](https://doi.org/10.1016/S0305-0548(97)00031-2)  
588 22. Hansen P, Mladenović N. (1999). An Introduction to Variable Neighborhood Search. In: Voß,  
589 S., Martello, S., Osman, I.H., Roucairol, C. (eds) Meta-Heuristics. Springer, Boston, MA.  
590 [https://doi.org/10.1007/978-1-4615-5775-3\\_30](https://doi.org/10.1007/978-1-4615-5775-3_30)  
591 23. Chen A, Liao S, Cheng M, Ma K, Wu L, Lai Y, et al. Spatiotemporal transcriptomic atlas of  
592 mouse organogenesis using DNA nanoball-patterned arrays. Cell 2022;185(10):1777–1792.  
593 24. Maynard KR, Collado-Torres L, Weber LM, Uytingco C, Barry BK, Williams SR, et al.  
594 Transcriptome-scale spatial gene expression in the human dorsolateral prefrontal cortex.  
595 Nature neuroscience 2021;24(3):425–436.  
596 25. Shen R, Liu L, Wu Z, Zhang Y et al. (2022). Data from: Application of Spatial-ID to large field  
597 mouse brain hemisphere dataset measured by Stereo-seq [Data set]. Zenodo.  
598 <https://doi.org/10.5281/zenodo.7340795>  
599 26. STOMICS database MOSTA download <https://db.cngb.org/stomics/mosta/download/>  
600 27. Spatial LIBD GitHub <https://github.com/LieberInstitute/spatialLIBD>  
601 28. Hubert L, Arabie P. Comparing partitions. Journal of Classification 1985; 2: 193–218.  
602 29. Djordjevic A; Li J; Fang S; Cao L; Ivanovic M (2024): Supporting data for "A Novel Variable  
603 Neighborhood Search Approach for Cell Clustering for Spatial Transcriptomics" GigaScience  
604 Database. <http://dx.doi.org/10.5524/102498>  
605